R measurements (resistivity, magnetoresistance, Hall).

590B

Makariy A. Tanatar

April 18, 2014

Resistivity

Typical resistivity temperature dependence:

metals, semiconductors

Magnetic scattering

Resistivities of Real Materials

Material	Resistivity 20°C
Silver	1.59 μΩ cm
Copper	1.72 μΩ cm
Aluminum	2.82 μΩ cm
Tungsten	5.8 μΩ cm
Platinum	11 μΩ cm
Manganin	48 μΩ cm
Constantan	49 μΩ cm
Nichrome	110 μΩ cm
Germanium	4.6
Glass	10^{8}-10^{12} Ω cm
PET	10^{18} Ω cm
Teflon	10^{20}-10^{22} Ω cm

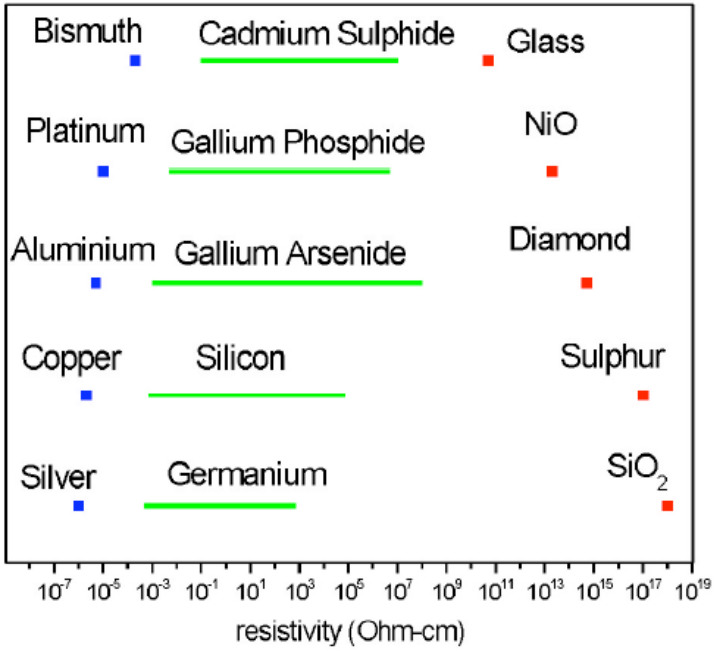

Most semiconductors in their pure form are not good conductors, they need to be doped to become conducting.

Not all so called "ionic" materials like oxides are insulators.

- We can relate the conductivity, σ, of a material to microscopic parameters that describe the motion of the electrons (or other charge carrying particles such as holes or ions).

$$\sigma = ne(e\tau/m^*)$$

$$\mu = e\,\tau\,/m^*$$

$$\sigma = ne\,\mu$$

- where
- n = the carrier concentration (cm^{-3})
- e = the charge of an electron = 1.602×10^{-19} C
- τ = the relaxation time (s) {the time between collisions}
- m* = the effective mass of the electron (kg)
- μ = the electron mobility ($cm^2/V\text{-}s$)

Metals, Semiconductors & Insulators

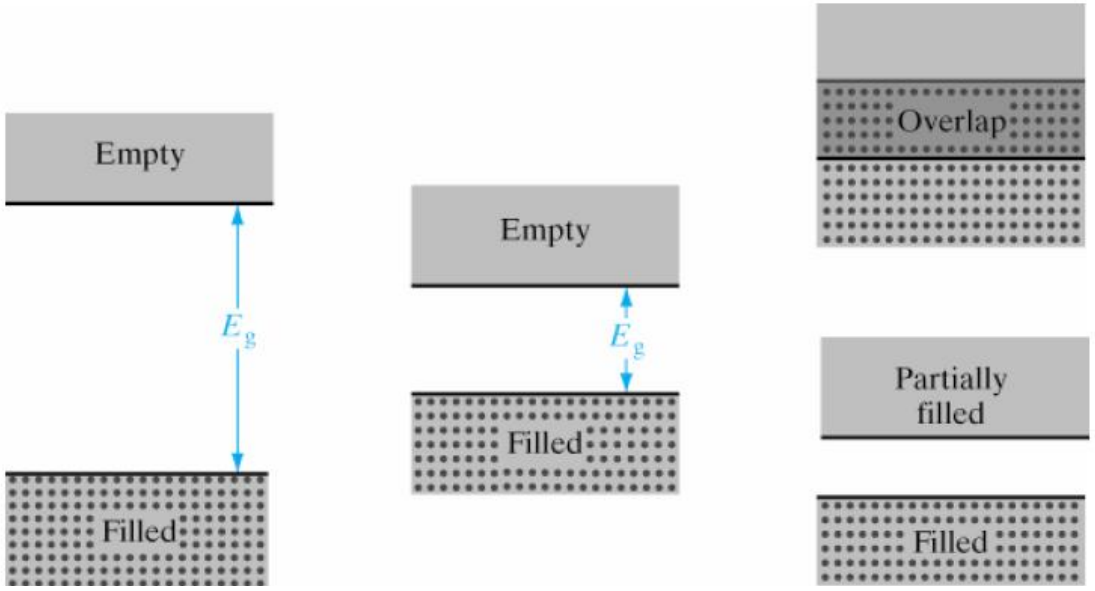

Insulator Semiconductor Metal

Big variation is due to big difference in free carrier density

Energy bands in semiconductors

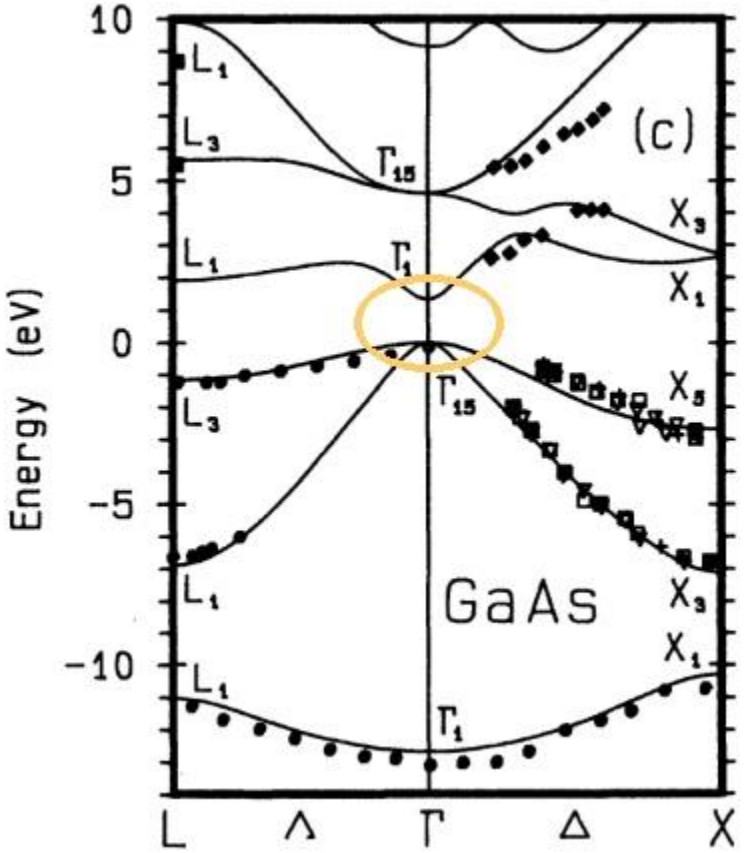

Direct-gap
III-V
II-VI

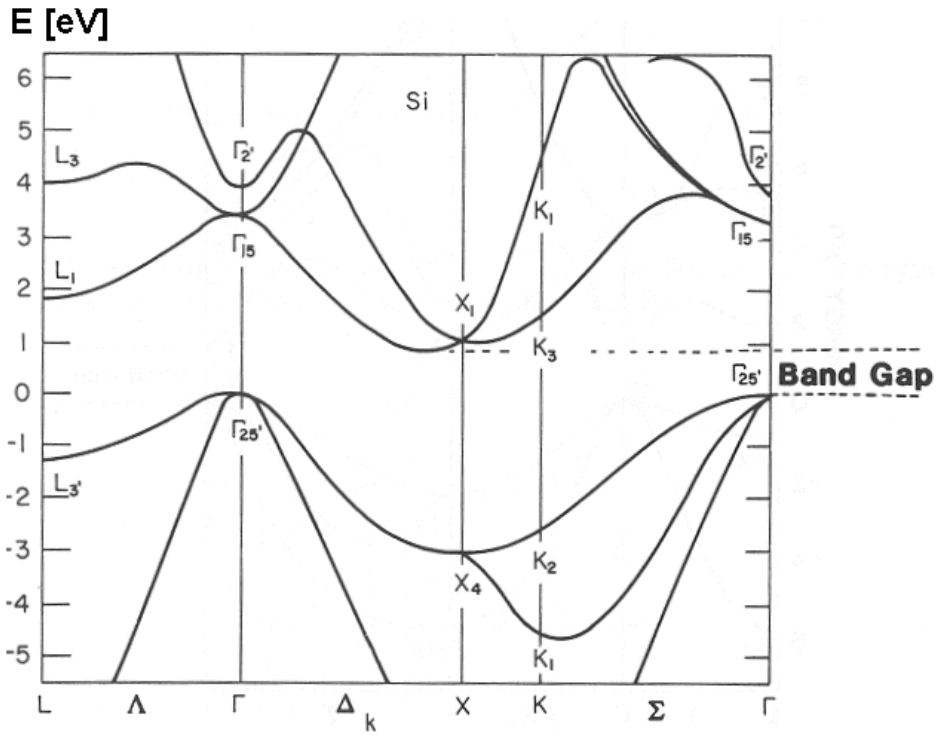

Indirect band-gap
Si, Ge

Compound	Structure	Bandgap (eV)	e^- mobility (cm^2/V-s)	h^+ mobility (cm^2/V-s)
Si	Diamond	1.11 (I)	1,350	480
Ge	Diamond	0.67 (I)	3,900	1,900
AlP	Sphalerite	2.43 (I)	80	---
GaAs	Sphalerite	1.43 (D)	8,500	400
InSb	Sphalerite	0.18 (D)	100,000	1,700
AlAs	Sphalerite	2.16 (I)	1,000	180
GaN	Wurtzite	3.4 (D)	300	---

Electron mobility and scattering

What scatters carriers?

Disruptions in periodicity

- defects
- lattice vibrations
- surfaces

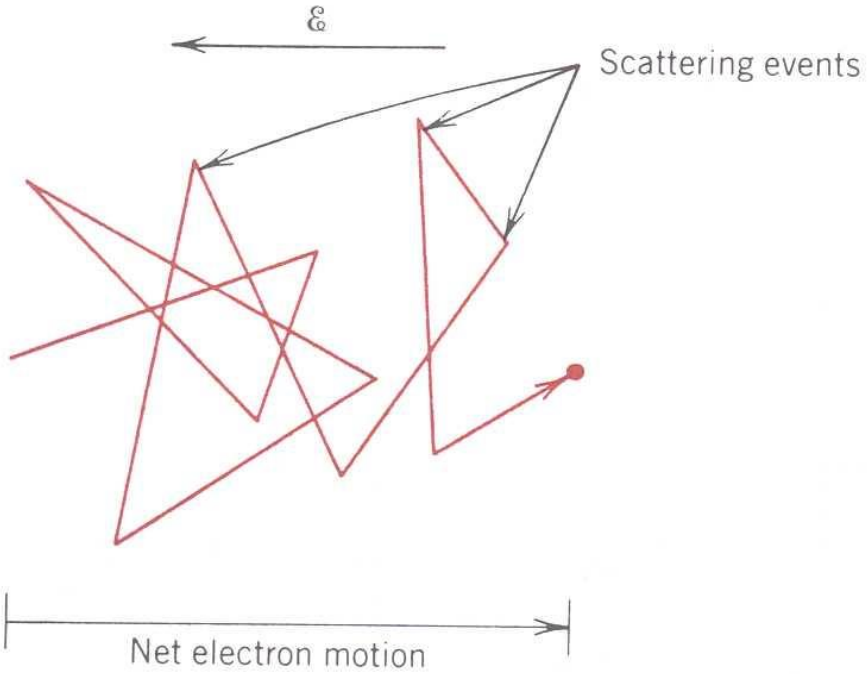

- ***Thermal energy*** $\Rightarrow$ some electrons are excited from the valence band into the conduction band $\Rightarrow$ ***conduction electrons***
- This leaves an empty state in the valence band — a ***hole***
  - *n*: density of CE
  - *p*: density of holes

$$n \cdot p = N_C N_V \exp\left(-\frac{E_g}{k_B T}\right)$$

- Intrinsic semiconductor: electrons and holes form in pairs

$$n_i = p_i = \sqrt{N_C N_V}\exp\left(-\frac{E_g}{2k_B T}\right)$$

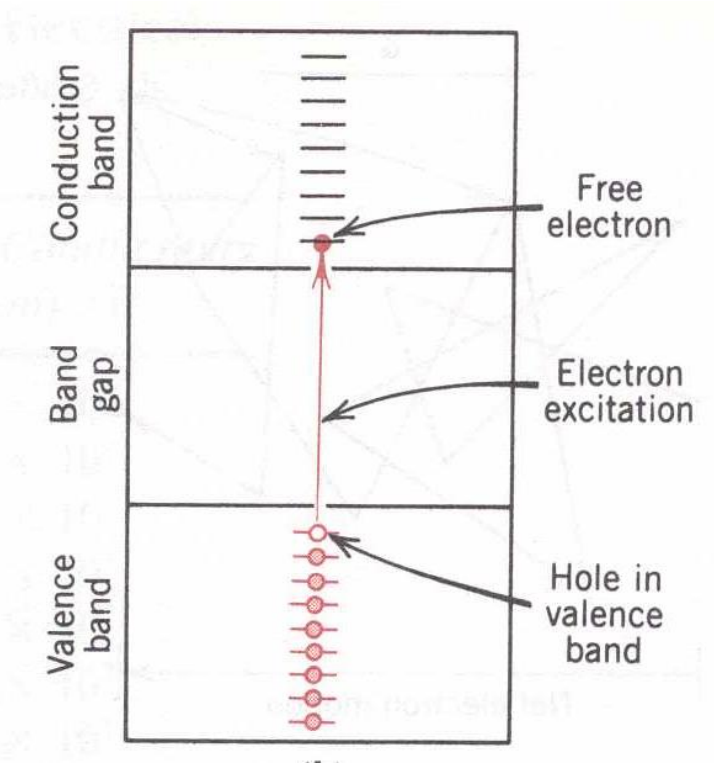

- Conductivity:

$$\sigma = n_i e\mu_e + p_i e\mu_h = n_i e(\mu_e + \mu_h)$$

Carrier density

- Low T: ***ionization*** of dopants
  - *n*-type: donor atoms donate e^- to conduction band
  - *p*-type: acceptor atoms accept e^- from valence band
- Intermediate T: all dopants ionized
  - *n*-type: ***exhaustion*** of donors
  - *p*-type: ***saturation*** of acceptors
- High T: intrinsic behavior

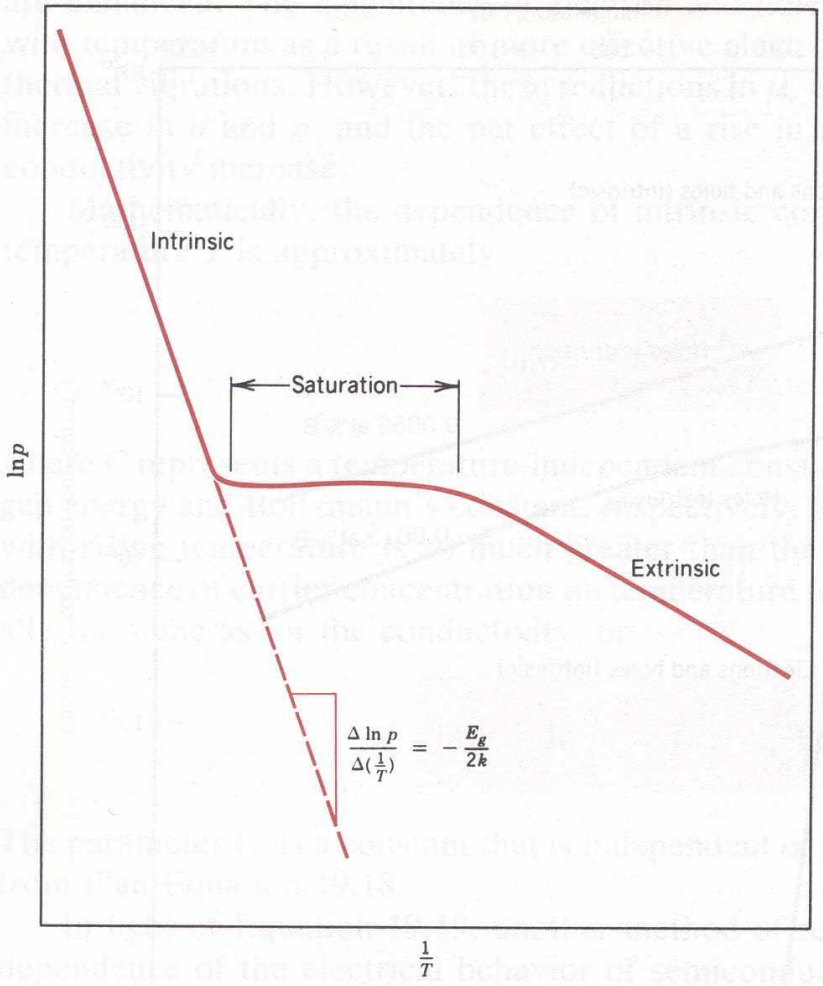

Schematic plot of the natural logarithm of hole concentration as a function of the reciprocal of absolute temperature for a *p*-type semiconductor that exhibits extrinsic, saturation, and intrinsic behavior.

Can obtain bandgap for intrinsic region

$$n = p = \sqrt{N_C N_V}\exp\left(-\frac{E_g}{2k_B T}\right)$$

Intrinsic

If density of dopants N>>n,p
Behaves like extrinsic conductor

Extrinsic

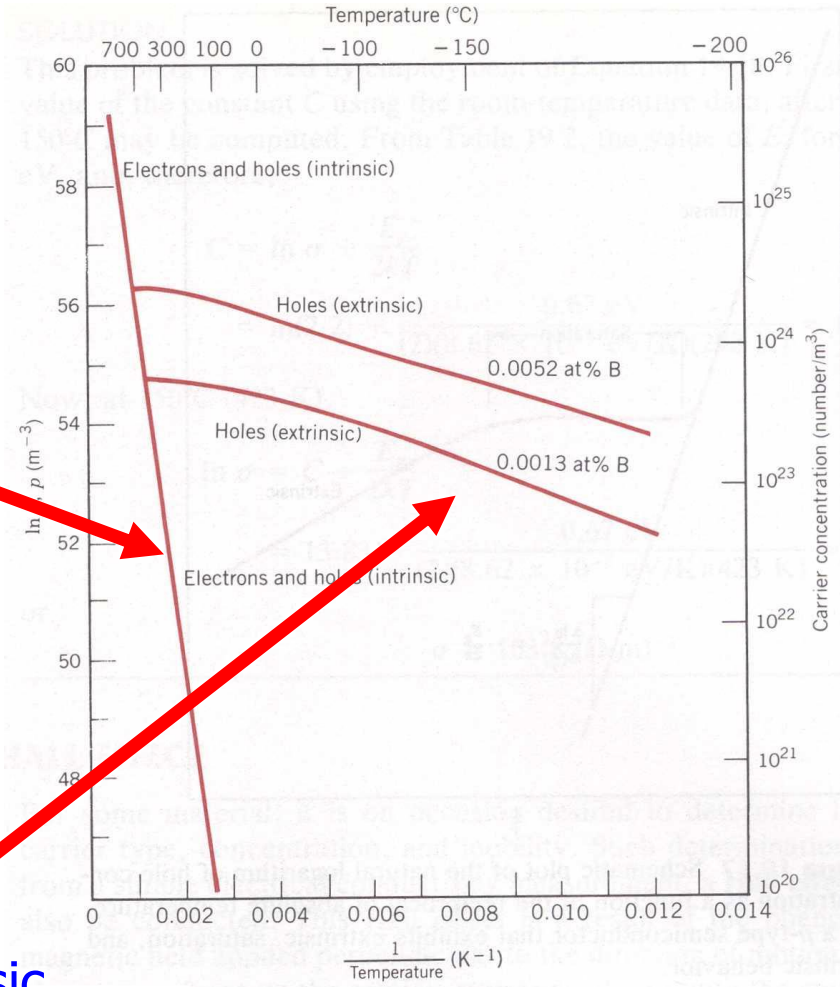

The logarithm of carrier (electron and hole) concentration as a function of the reciprocal of the absolute temperature for intrinsic silicon and two boron-doped silicon materials. (Adapted from G. L. Pearson and J. Bardeen, *Phys. Rev.*, **75**, 865, 1949.)

$$\sigma = ne\mu_e + pe\mu_h \cong ne\mu_e = N_d e\mu_e$$

Metals

D. MATTHIESSEN'S RULE $R = R_0 + R_T$,

$$\rho - \rho_0 = \rho_0 \alpha (T - T_0)$$

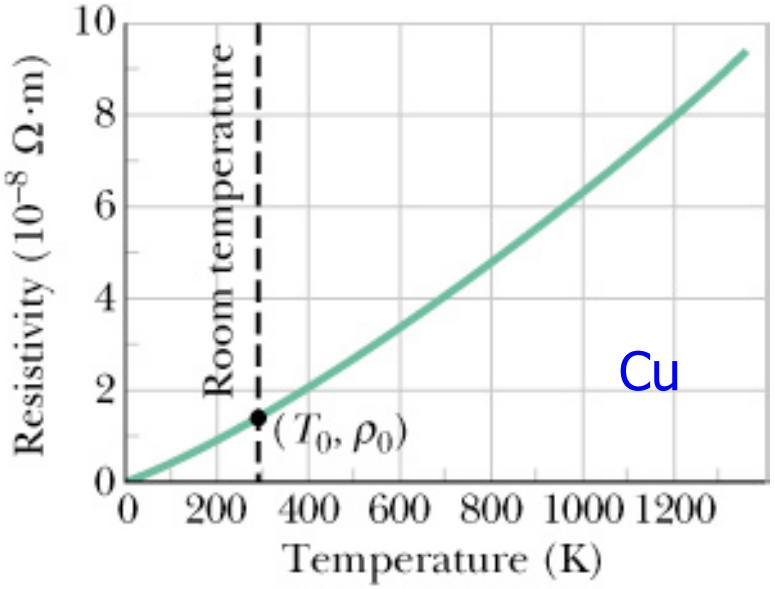

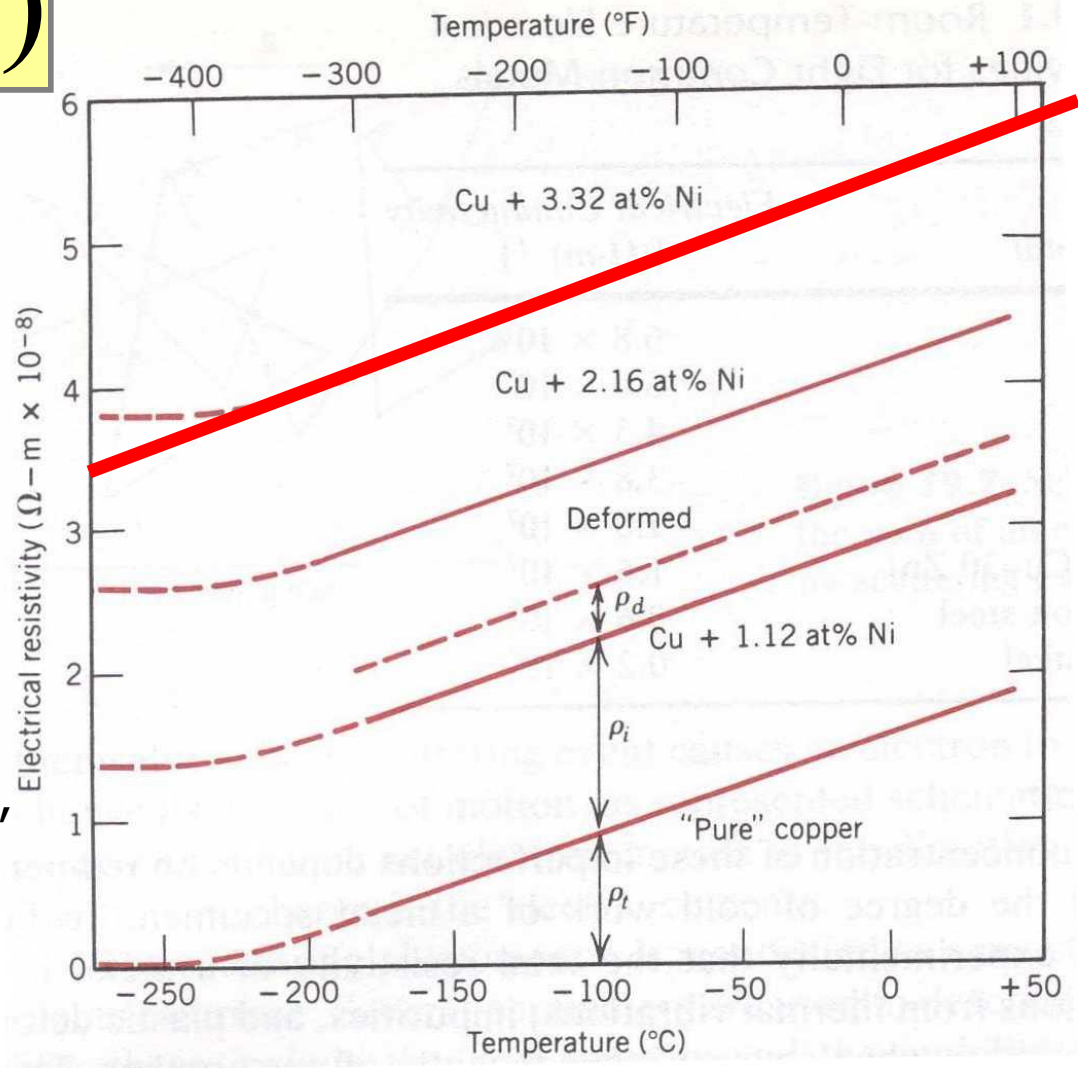

Temperature coefficient of resistivity α reflects electron-phonon interaction, property of material

- Thermal vibrations scatter carriers
- $\Rightarrow$ mobility↓
  $\Rightarrow$ conductivity↓
  $\Rightarrow$ resistivity↑

D. Matthiessen's Rule

$$R = R_0 + R_T,$$

- Effect of ***impurities*** on μ

$$\rho_i = A c_i (1 - c_i)$$

- A: property of host and impurity
- c_i: atomic fraction of impurity

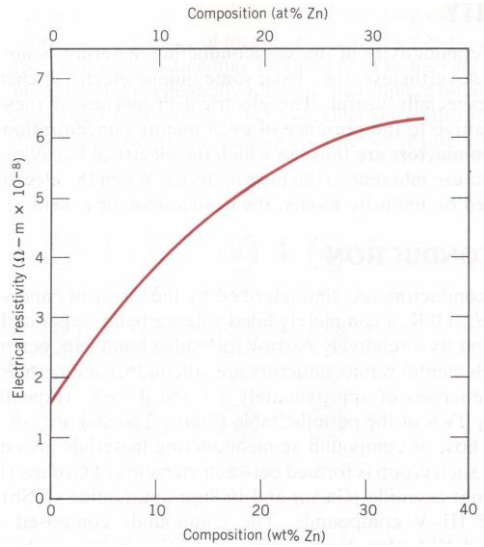

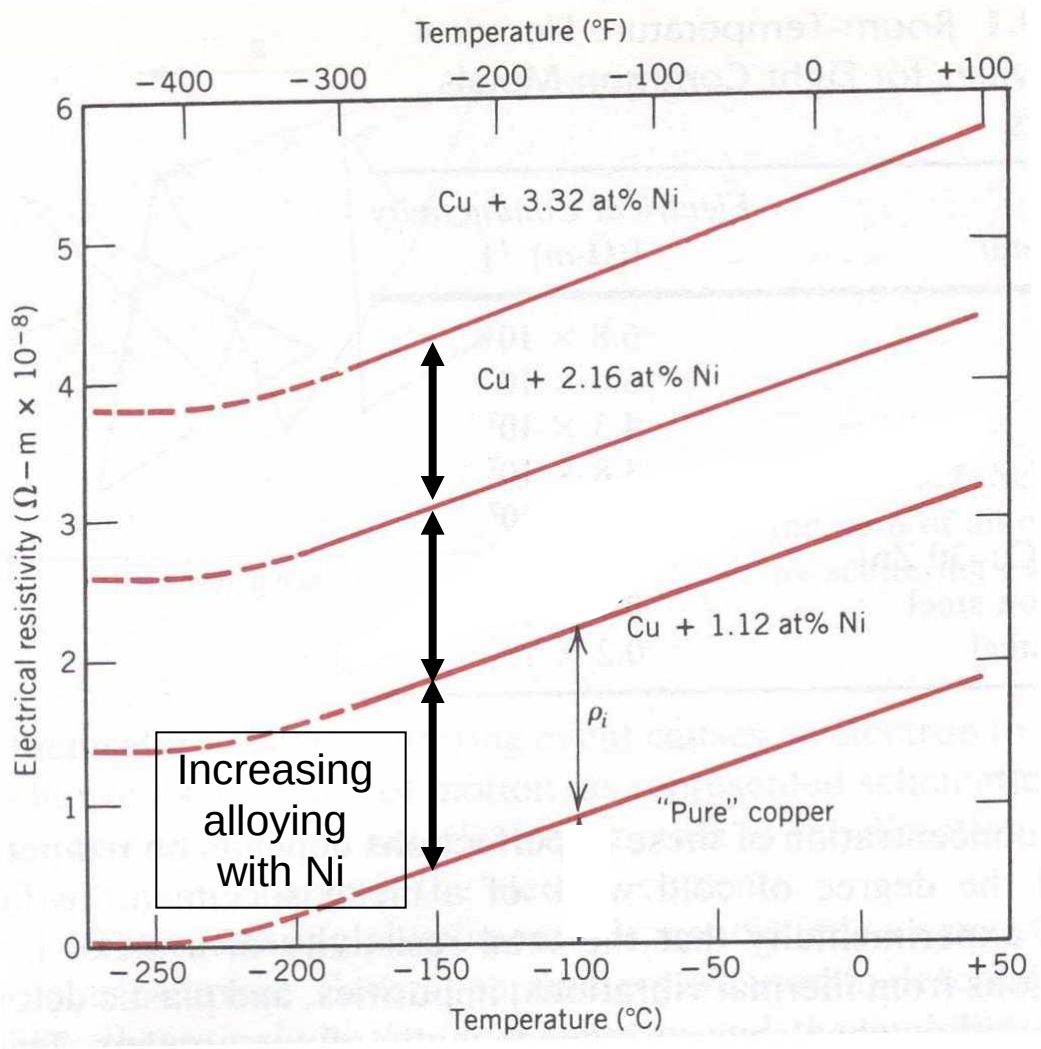

- Effect of ***deformation*** on μ
  - Dislocations (regions of deformed material) scatter carriers, increasing the electrical resistivity by ρ_D

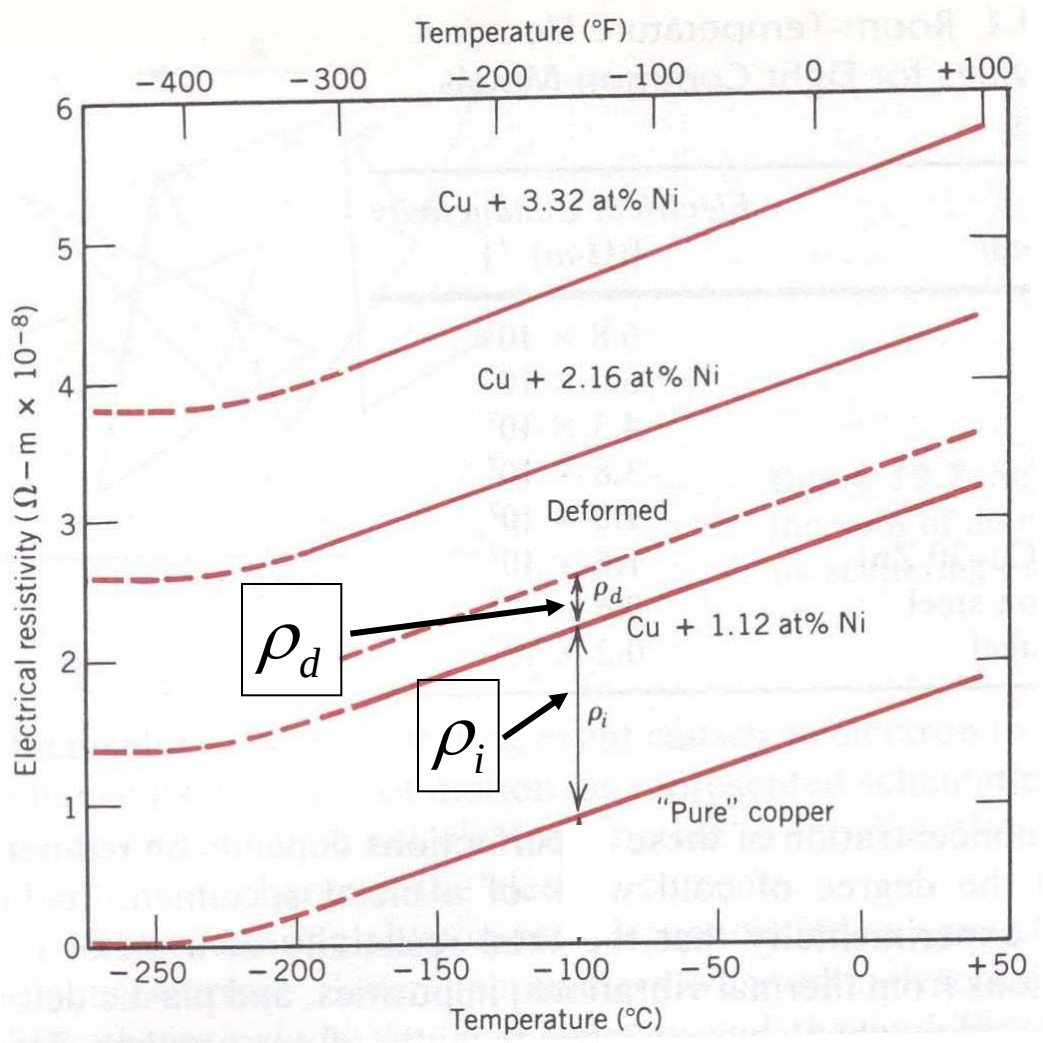

Resistivity temperature dependence of metals closer look

High temperature

$$\rho - \rho_0 = \rho_0 \alpha \left(T - T_0 \right)$$

$T >> \Theta_D$ density of phonons ~T

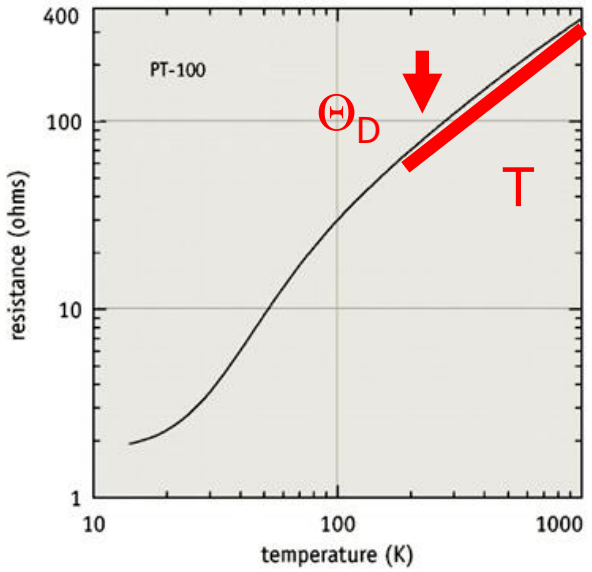

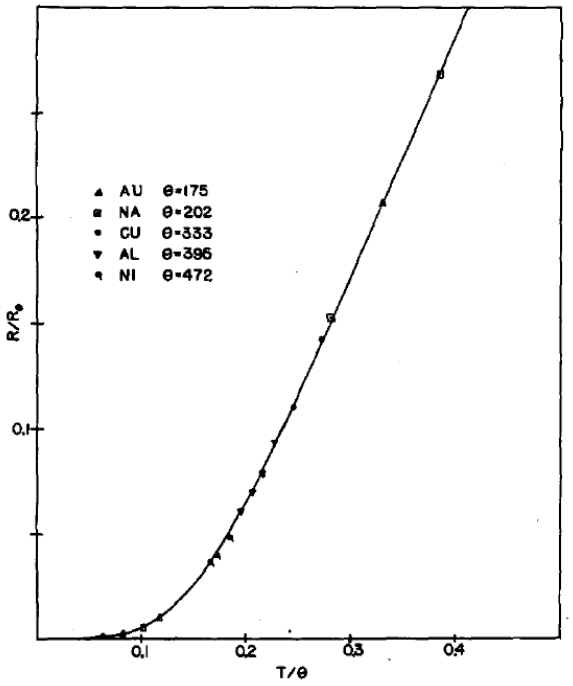

FIG. 1. Temperature variation of resistance of various metals. The curve is a plot of the Bloch-Gruneisen function (Eq. (28)). Data from values quoted by Meissner (cf. Bibliography).

$T < \Theta_D$ spectrum of phonons changes

Bloch-Gruneisen law

For most of metals

$R = R_0 f(T/\Theta)$,

Θ is close to Debye temperature

in specific heat, not the same due to selectivity of scattering

$$\rho(T) = \rho(0) + A \left(\frac{T}{\Theta_R} \right)^n \int_0^{\frac{\Theta_R}{T}} \frac{x^n}{(e^x - 1)(1 - e^{-x})} dx$$

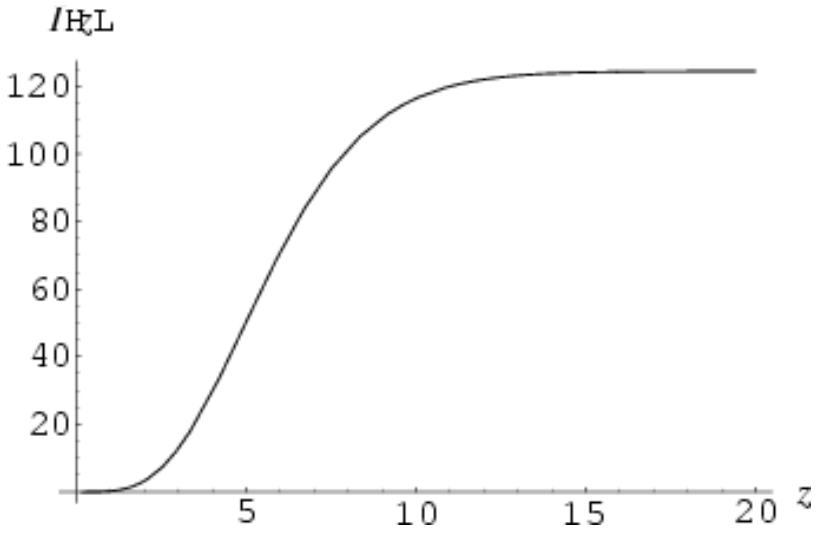

xT

$\rho_{ph} \sim f(q) S_{ph}$

With some "filtering" due to q-dependence of scattering probability

Comparison of Θ_R and Θ_D

Metal	Ag	Au	Al	Cu	Pd	Pt	Rh
Θ_R	200	200	395	320	270	240	340
Θ_D	220	185	385	320	300	225	350

After G. T. Meaden Electrical Resistance of Metals

q=0 at T=0

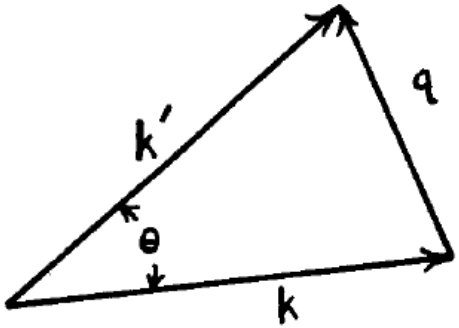

FIG. 11. Illustrating the vector relations for the scattering of an electron wave by a lattice wave.

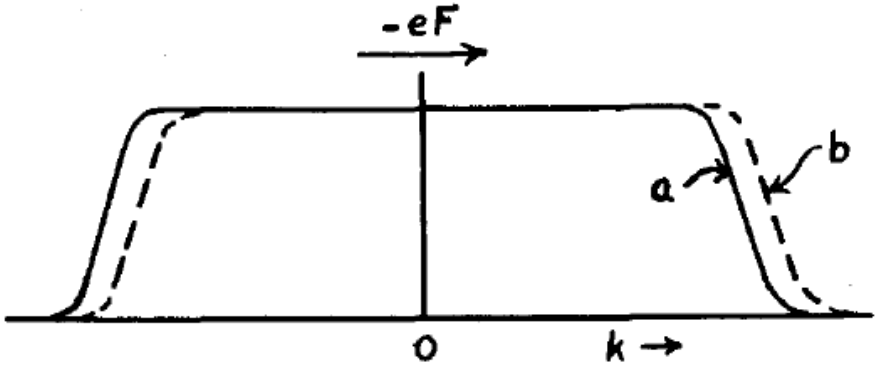

FIG. 9. Shift of the electron distribution due to an applied field.

Direct electron scattering on phonons at low temperatures does not contribute much to resistivity, electrons can not scatter at large angle due to momentum conservation law

The only efficient way: Umklapp processes, scattering with momentum transfer to reciprocal lattice

Umklapp processes

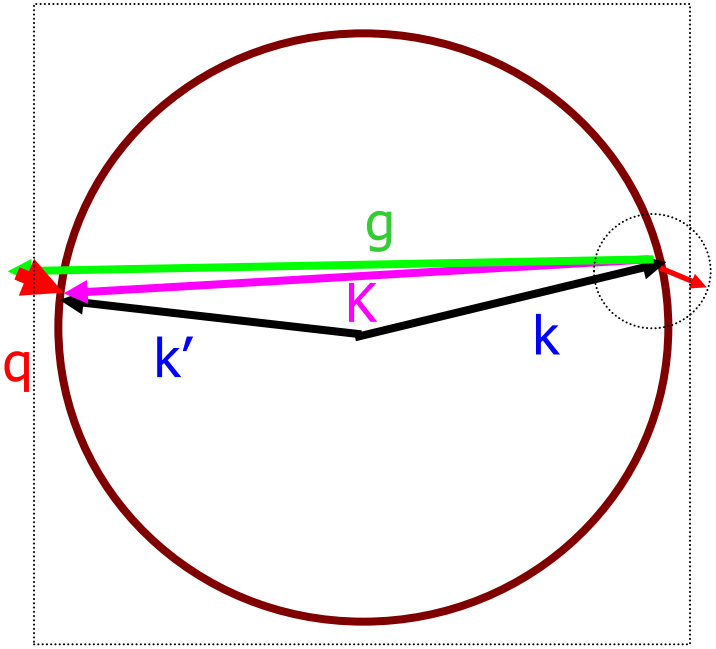

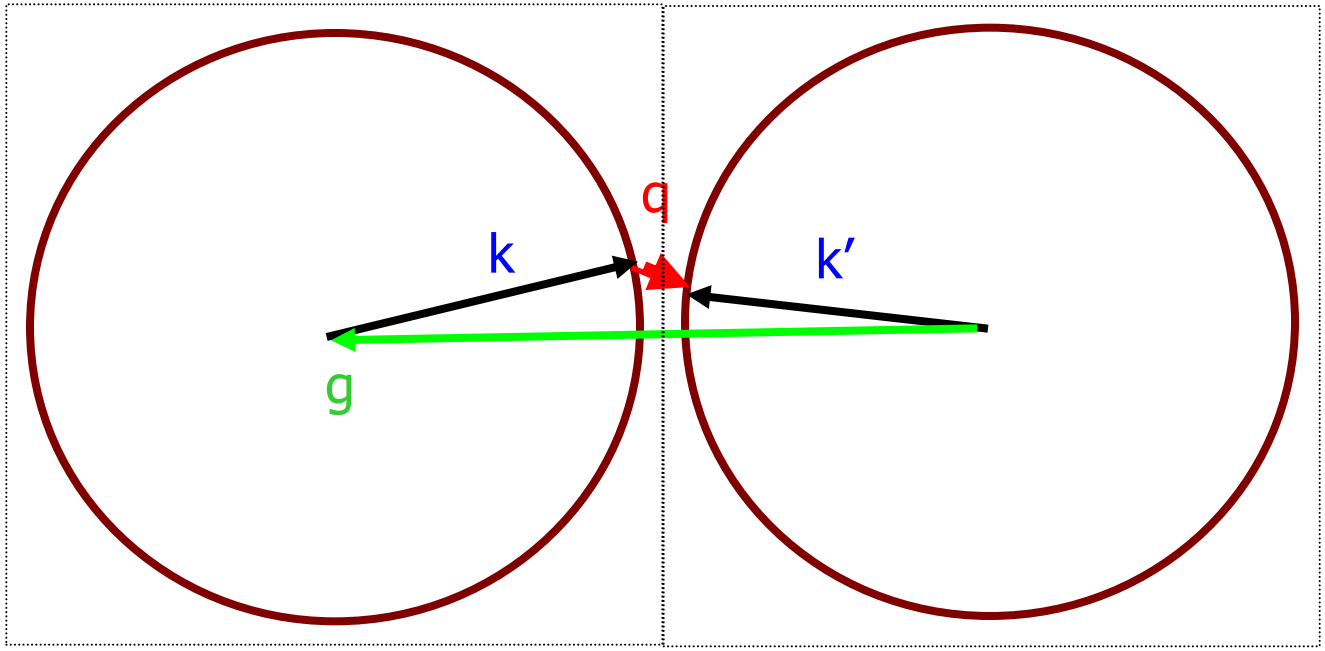

Electron-electron scattering

At low temperatures

$\rho=\rho_0+\alpha T^n$

n=5 e-ph

Not very efficient in scattering

In e-e scattering total momentum is conserved

Scattering does not contribute to resistivity

•Umklapp

•Electrons from different bands

s-d scattering

$$\sigma = (Ne^2/m)(\alpha\tau_a + \beta\tau_b).$$

Bands a and b, densities α and β

Relaxation times τ_a and τ_b

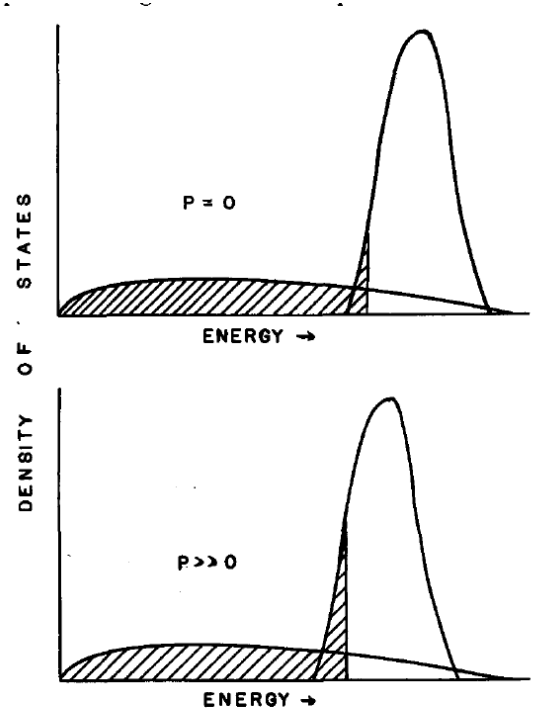

FIG. 14. Occupied electronic states in two overlapping bands at (a) zero pressure, (b) some high pressure (schematic).

Mott: τ_a and τ_b are of the same order of magnitude;

$\alpha$and β can be very different,

High probability of scattering into large DOS band

n=2 e-e

n=3 s-d

Kondo effect

Dilute magnetic impurities in metals

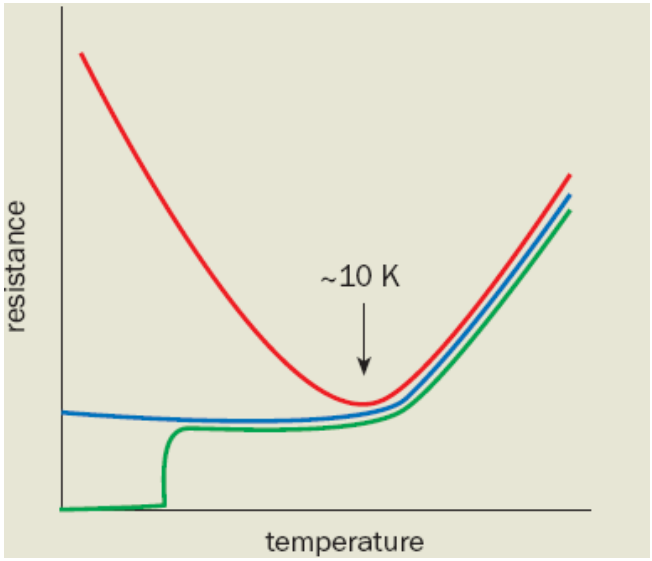

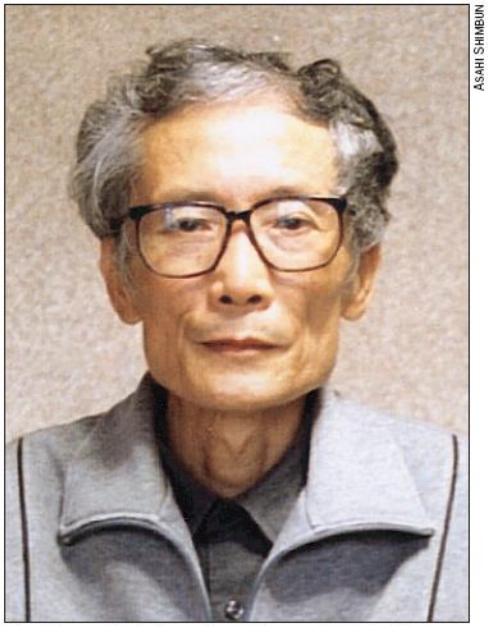

The theory that describes the scattering of electrons from a localized magnetic impurity was initiated by the work of Jun Kondo in 1964

b. 1930

Interaction of conduction electrons with magnetic impurities

Characteristic temperature T_K (varies a lot! From 0.1mK Mn in Au to 300K V in Au, usually ~10 K)

Specific heat per impurity C~T/TK
Impurity spins completely screened at low temperatures

Revival of the Kondo effect

Leo Kouwenhoven and Leonid Glazman

PHYSICS WORLD JANUARY 2001

Journal of the Physical Society of Japan
Vol. 74, No. 1, January, 2005, pp. 1–3

Anderson impurity model

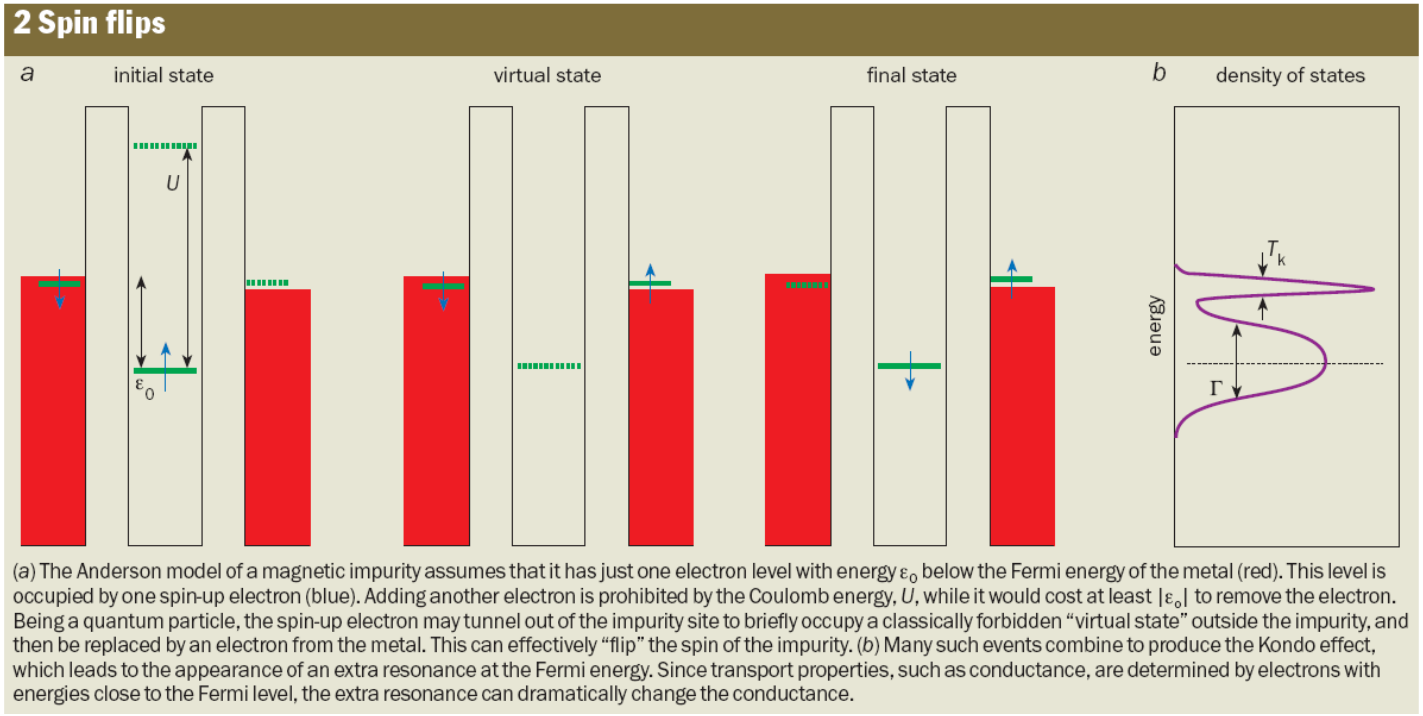

(a) The Anderson model of a magnetic impurity assumes that it has just one electron level with energy ε_0 below the Fermi energy of the metal (red). This level is occupied by one spin-up electron (blue). Adding another electron is prohibited by the Coulomb energy, U, while it would cost at least $|\varepsilon_0|$ to remove the electron. Being a quantum particle, the spin-up electron may tunnel out of the impurity site to briefly occupy a classically forbidden "virtual state" outside the impurity, and then be replaced by an electron from the metal. This can effectively "flip" the spin of the impurity. (b) Many such events combine to produce the Kondo effect, which leads to the appearance of an extra resonance at the Fermi energy. Since transport properties, such as conductance, are determined by electrons with energies close to the Fermi level, the extra resonance can dramatically change the conductance.

Peak in DOS
Bound to E_F
additional scattering

$\rho/\rho_0 = f(T/T_K)$
universal function of one parameter T_K

$\rho \sim \ln T$

Revival of the Kondo effect
Leo Kouwenhoven and Leonid Glazman
PHYSICS WORLD JANUARY 2001

Magnetic scattering

$Ce_{1-x}La_xRhIn5$
f-electrons are localized

Same lattice
localized f-electrons
add to scattering

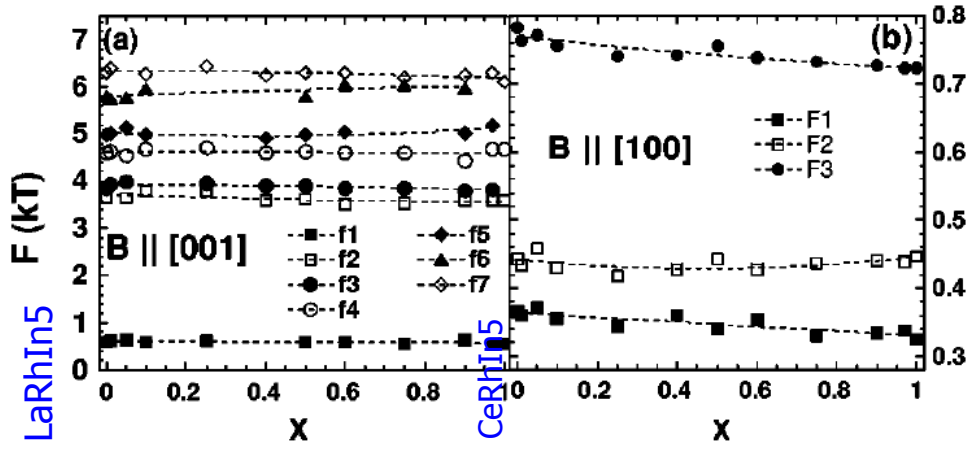

FIG. 2. The principal dHvA frequencies in $Ce_xLa_{1-x}RhIn_5$ plotted versus x, (a) for B applied along [001] and (b) for B applied along [100].

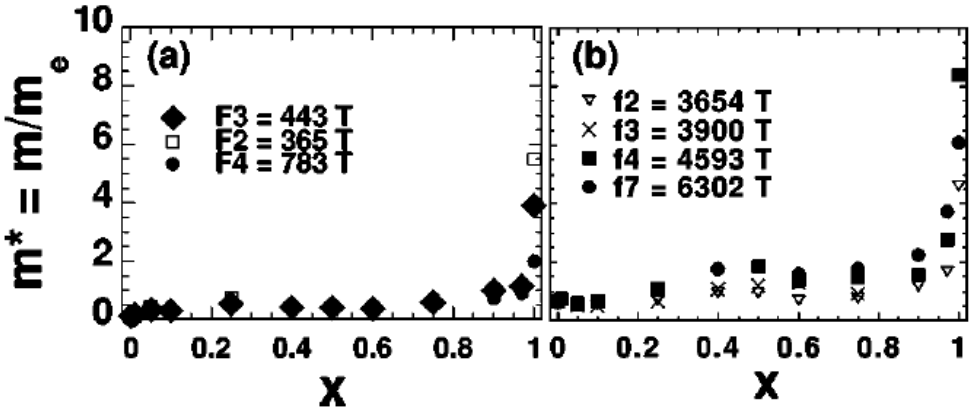

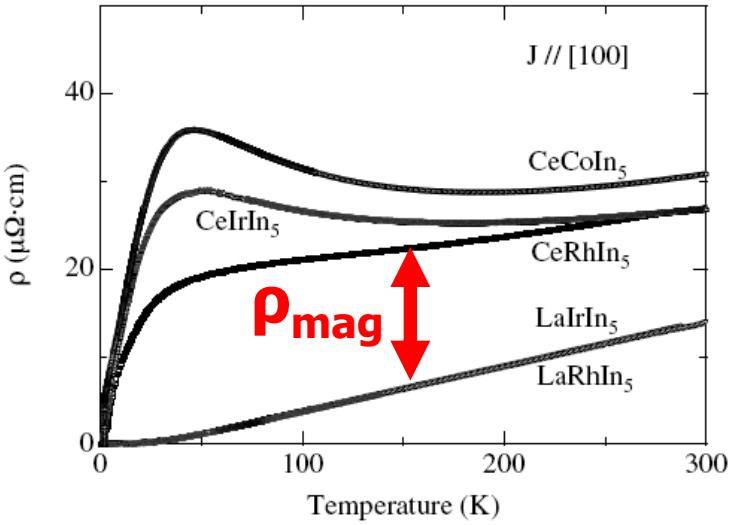

Fig. 3. Temperature dependence of the electrical resistivity in $RTIn_5$.

CeRhIn5

$\rho_{mag} \sim S_{mag}$

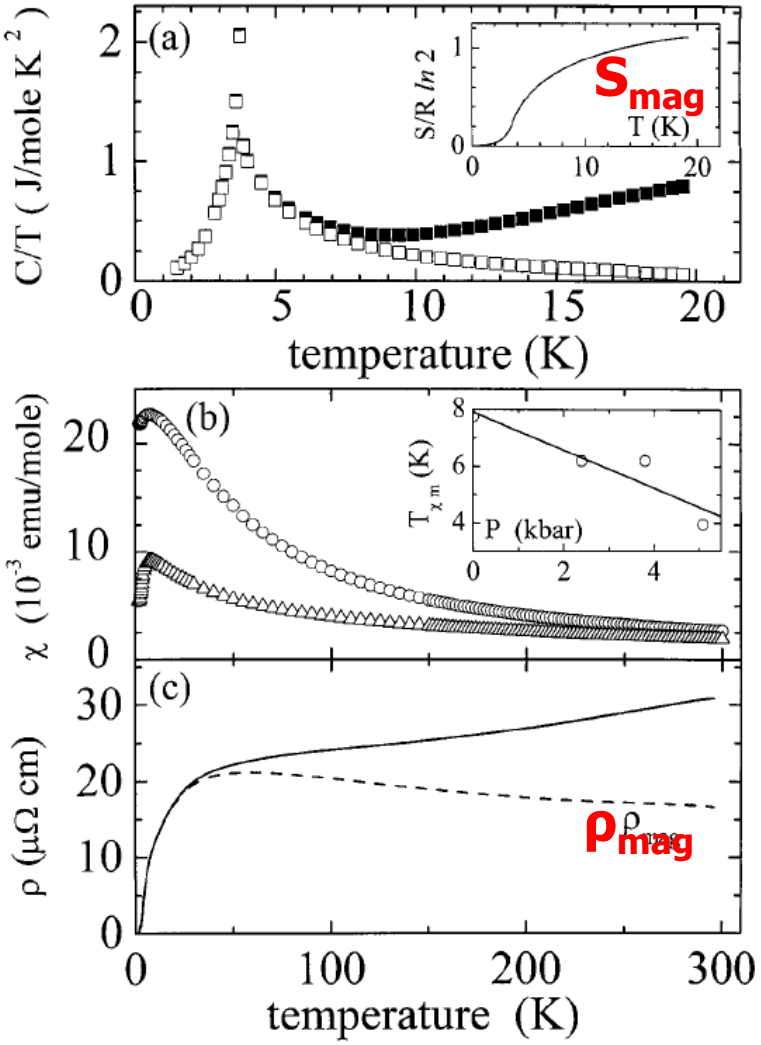

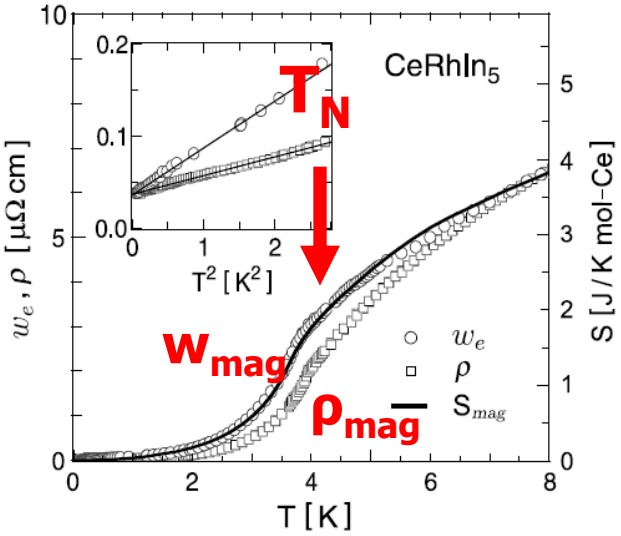

FIG. 2. Electronic thermal resistivity w_e (circles) and electrical resistivity ρ (squares), compared to the magnetic entropy S_{mag} (line) obtained from published specific heat data [12]. Inset: low-temperature data as a function of T^2. Lines are linear fits.

"q-filtering" removed:
Full scattering directly proportional to entropy

Density waves

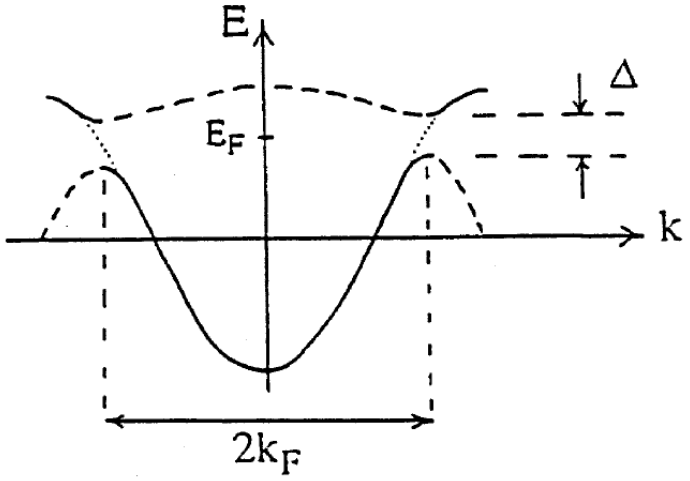

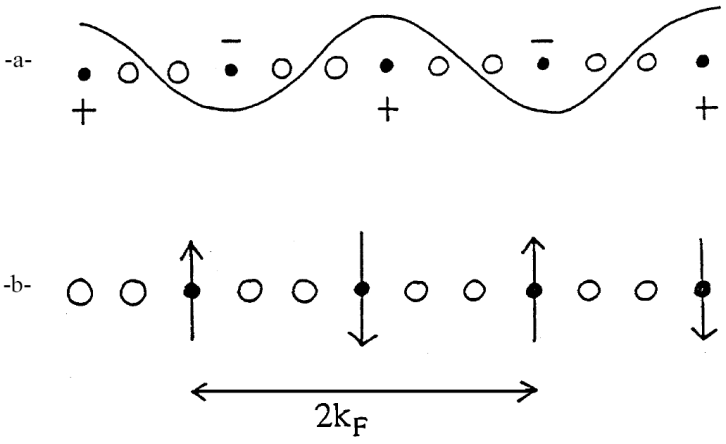

Distortion with $2K_F$ periodicity
Decreases electron energy

Rudolph Peierls
1907-1995

"Frisch-Peierls Memorandum" of March 1940, proposing a "super-bomb which utilizes the energy stored in atomic nuclei as a source of energy."
1957 on request of US government removed security clearance, suspected of spying

Klaus Fuchs

knighted in 1968

www.history.bham.ac.uk/research/index.htm

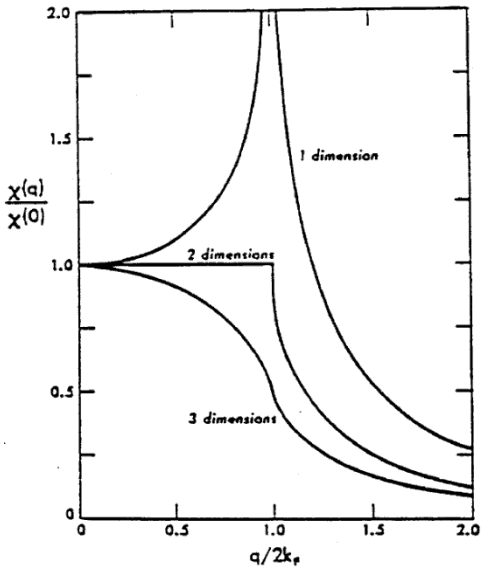

BCS-like solution
Δ=1.75 Tc

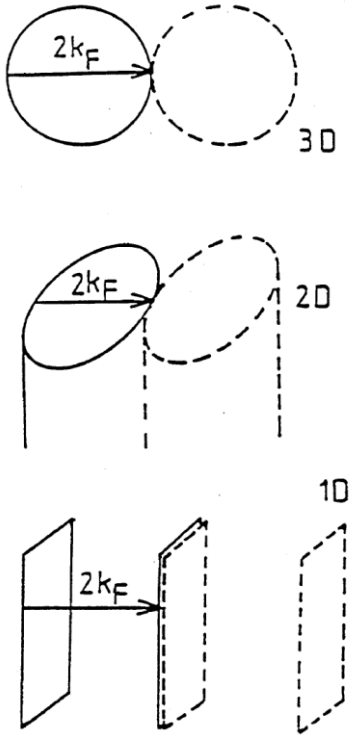

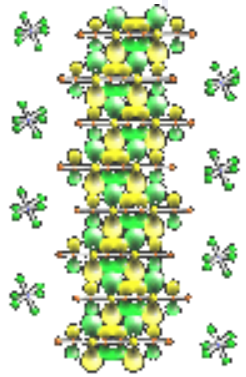

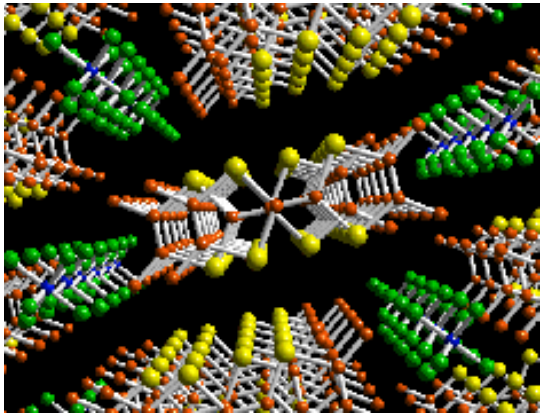

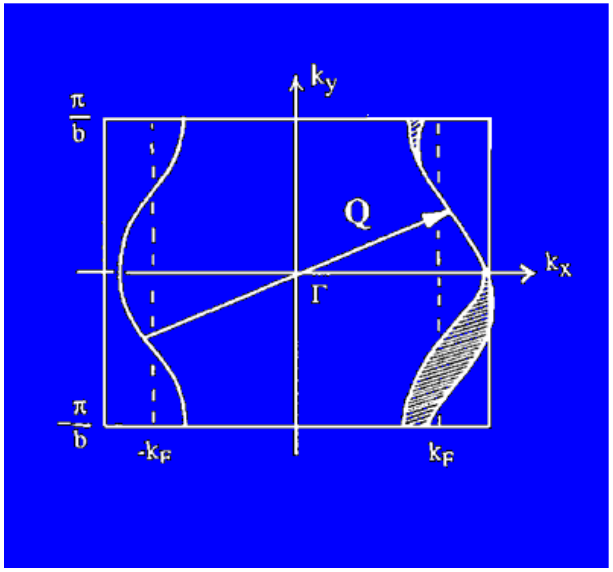

The Fermi surface of a quasi-1D conductor wo distinct parts at $+k_F$ and $-k_F$ (here in a cut view).
Q nest one part to another by translation.

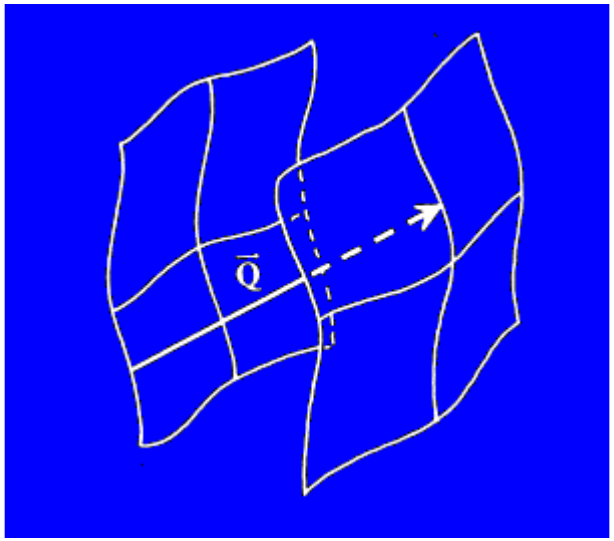

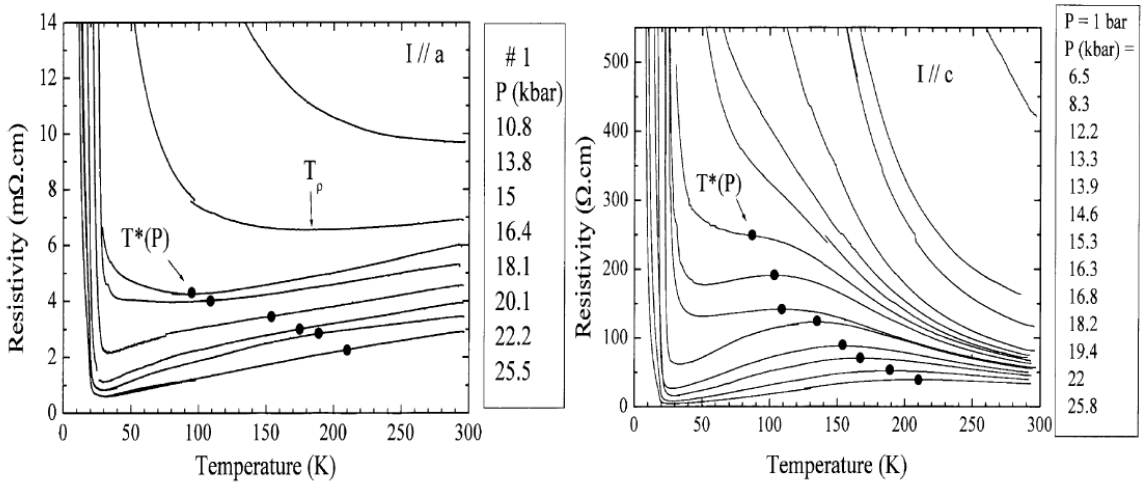

Fig. 2. $(TMTTF)_2PF_6$ longitudinal (left) and transverse (right) resistances versus temperature at different pressures.[12)]

Density waves: increasing dimensionality

Chain

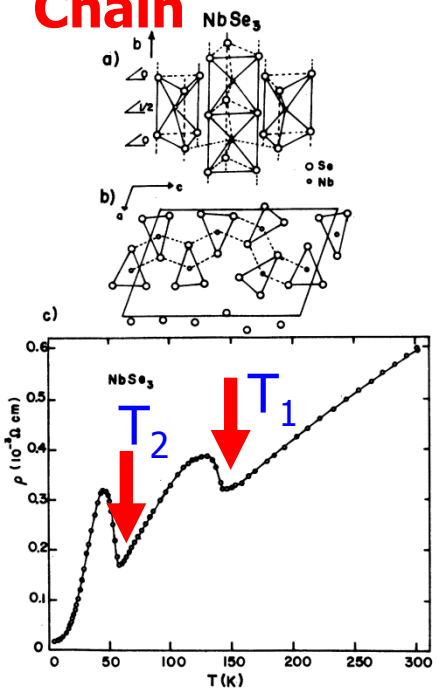

FIG. 1. (a) Crystal structure of $NbSe_3$ along the b axis. The Nb atoms in adjacent chains are displaced by half a lattice spacing along $\vec{b}$ with respect to each other. (b) Crystal structure of $NbSe_3$ in the a–c plane. The unit cell, comprised of six prisms and represented by the parallelogram, has the dimensions $a = 10.006$ Å, $b = 3.478$ Å, $c = 15.626$ Å, $\beta = 109.30°$. The Nb–Nb distance along $\vec{b}$ is 3.478 Å (compared to 2.68 Å in the metal). In the other directions it varies from 4.45 to 4.25 Å. The dashed lines connect Nb and Se atoms in the same plane. (c) Resistivity of $NbSe_3$ vs temperature. The phase transitions at 145 K and 59 K have been tentatively identified with the formation of charge-density waves.

NbSe3

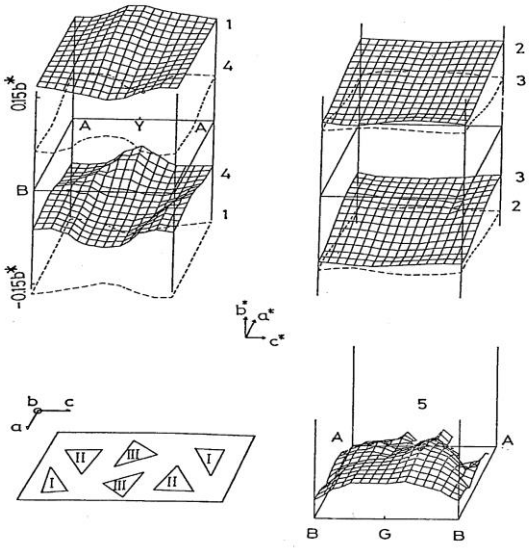

Fig. 1. Fermi surfaces corresponding to each conduction bands and the chain location in a unit cell of $NbSe_3$. The nesting pairs, 1–4 and 2–3, are pictured in half of the Brillouin zone. Each of the nesting pieces of the Fermi surfaces is drawn in the solid and dashed line. Fermi surface 5 is pictured in quarter of the Brillouin zone.

Layer

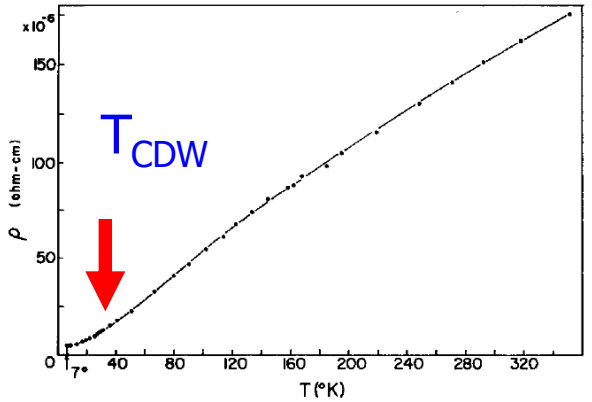

FIG. 1. The resistivity as a function of temperature for $NbSe_2$.

NbSe2

T1=142K ICDW1 $q1=(0.245\pm0.007)\ b^*$

T2=58K ICDW2 $q2(0.494\pm0.008)\ a^*+(0.267\pm0.007)\ b^*+0.50\ c^*$

Density-wave-Like

Anion ordering: big "external" periodic potential with periodicity close to $2K_F$

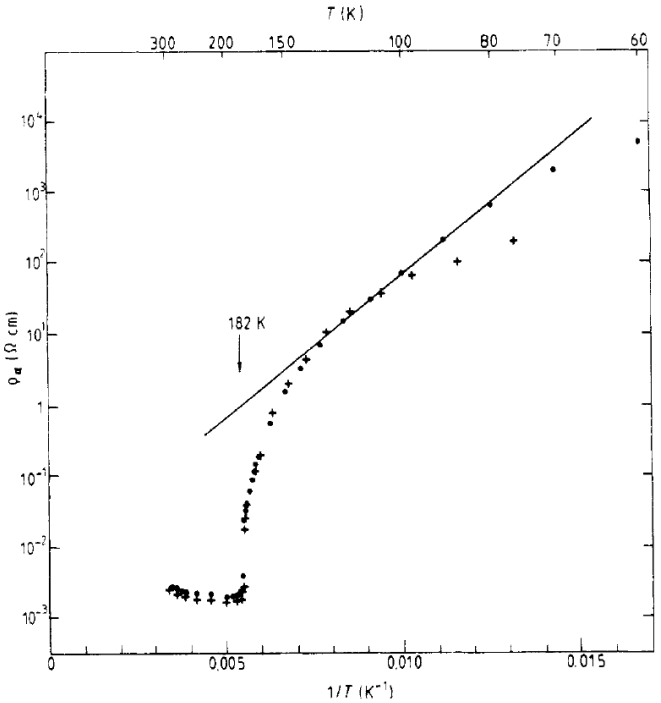

Figure 4. Logarithm of resistivity versus inverse temperature for $(TMTSF)_2ReO_4$ along the molecular stacks. Results are given for DC (full circles) and for 35 GHz (crosses).

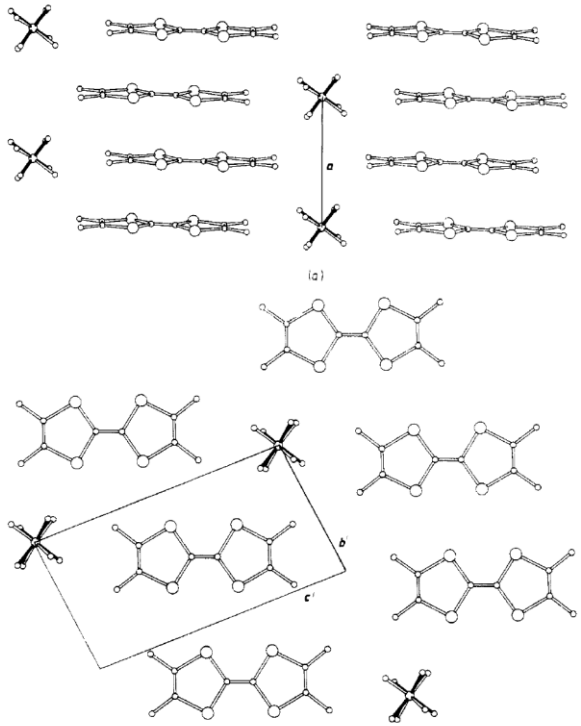

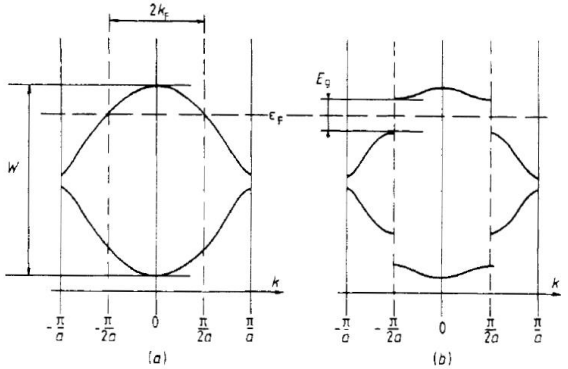

Figure 3. One-electron band structure of $(TMTSF)_2ReO_4$ shown schematically above (*a*) and below (*b*) the metal–insulator transition.

Almost all high-Tc materials have unusual ρ(T)
Electrons pair as they scatter!

PHYSICAL REVIEW B VOLUME 15, NUMBER 5 1 MARCH 1977

Apparent T^2 dependence of the normal-state resistivities and lattice heat capacities of high-T_c superconductors*

G. W. Webb, Z. Fisk, and J. J. Engelhardt
Institute for Pure and Applied Physical Sciences, University of California, San Diego, La Jolla, California 92093

S. D. Bader
Argonne National Laboratory, Argonne, Illinois 60439

(Received 8 March 1976; revised manuscript received 17 September 1976)

We report new measurements of the normal-state electrical resistances of several high-T_c (~20 K) A-15 structure superconductors. It is found that the resistances are linear functions of T^2 from T_c to 40 K. Analysis of available lattice heat-capacity data on the same materials shows that it also varies as T^2 over the same temperature interval. These observations suggest that the T^2 resistivity is due to electron-phonon scattering. This interpretation is supported by the results of a model calculation for the temperature dependence of the resistivity and the lattice-heat capacity of Nb_3Sn.

A15

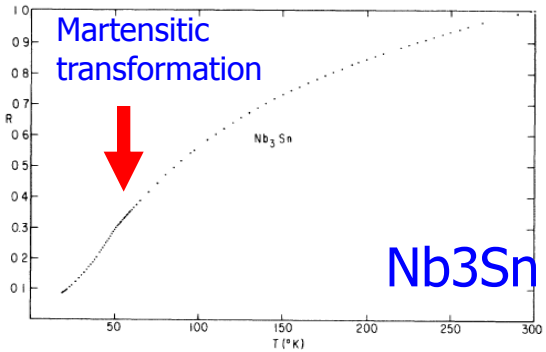

FIG. 1. Resistance of Nb_3Sn from T_c (18.2 K) to 300 K in units where R (300 K) = 1.0. The kink at 51 K is indicative of a martensitic transformation. Using the data of Woodward and Cody we estimate ρ (300 K) = 75 $\mu\Omega$ cm.

Strong electron-phonon interaction

Unusual ρ(T) dependence: saturation at high T,
Low T- extended range of T^2 behavior

Correlating with T^2 (rather than T^3)
lattice specific heat

VOLUME 69, NUMBER 20 PHYSICAL REVIEW LETTERS 16 NOVEMBER 1992

Systematic Evolution of Temperature-Dependent Resistivity in $La_{2-x}Sr_xCuO_4$

H. Takagi, B. Batlogg, H. L. Kao, J. Kwo, R. J. Cava, J. J. Krajewski, and W. F. Peck, Jr.
AT&T Bell Laboratories, Murray Hill, New Jersey 07974
(Received 8 May 1992)

$La_{2-x}Sr_xCuO_4$

X=0 – 0.15

X=0.1 – 0.35

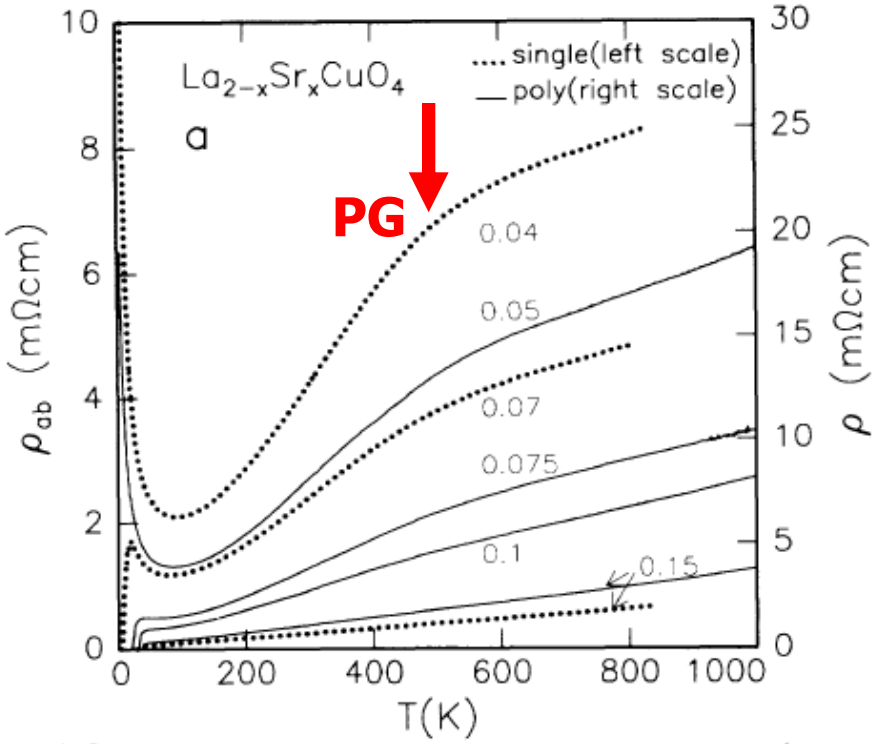

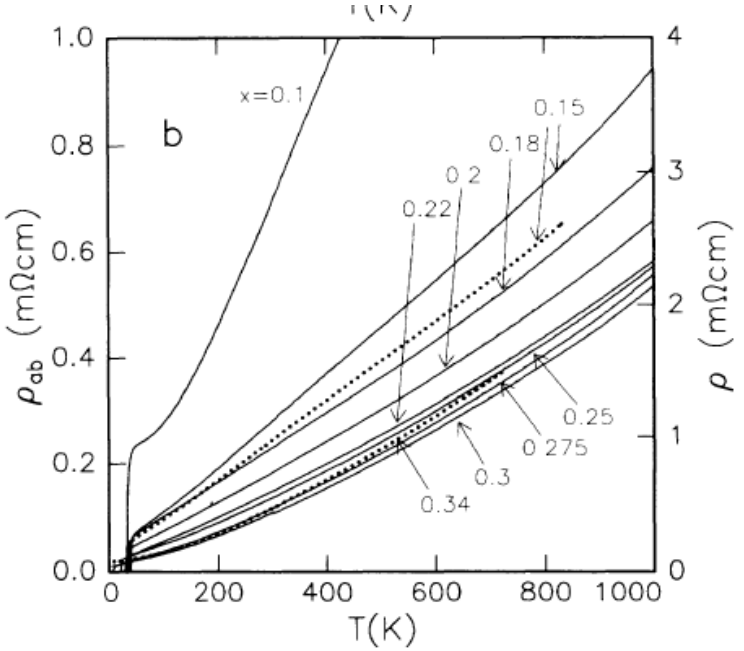

FIG. 1. The temperature dependence of the resistivity for $La_{2-x}Sr_xCuO_4$. (a) $0 < x \leq 0.15$, (b) $0.1 \leq x < 0.35$. Dotted lines, the in-plane resistivity (ρ_{ab}) of single-crystal films with (001) orientation; solid lines, the resistivity (ρ) of polycrystalline materials. Note, $\rho_M = (h/e^2)d = 1.7\ \mathrm{m}\Omega\,\mathrm{cm}$.

ρ~T at optimal doping
ρ~T^n at higher dopings

$La_{2-x}Sr_xCuO_4$ C-axis transport

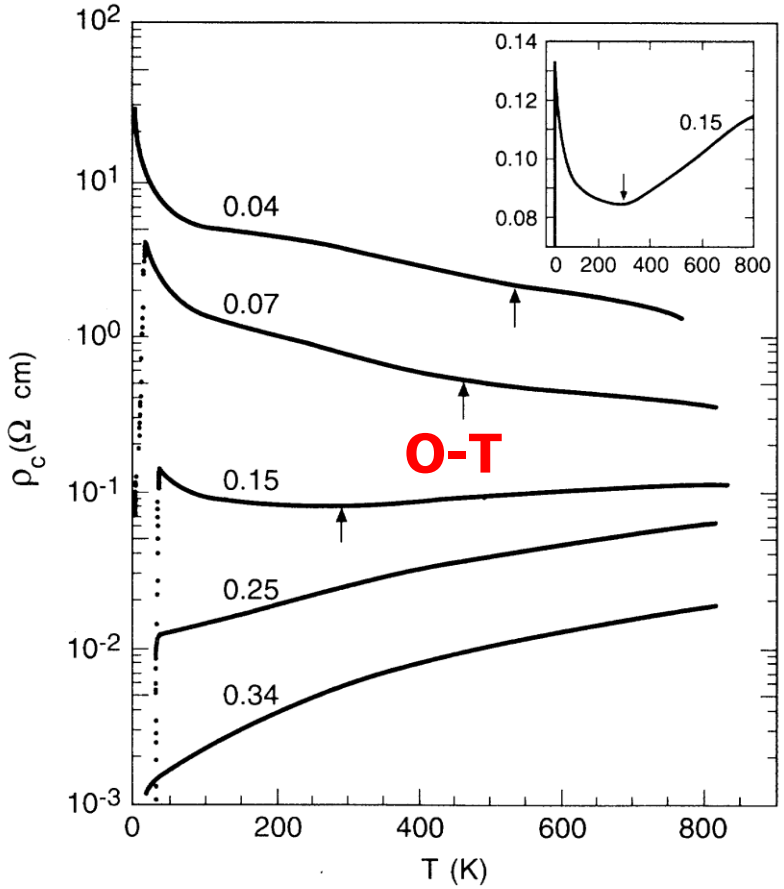

FIG. 3. Semilog plots of ρ_c vs T for $x = 0.04, 0.07, 0.15, 0.25,$ and 0.34. The inset shows the linear plot of ρ_c for $x = 0.15$. The arrows denote the temperature of the orthorhombic-to-tetragonal transformation where a discontinuous change of $d\rho_c/dT$ appears.

Highest Tc
heavy fermion CeCoIn5

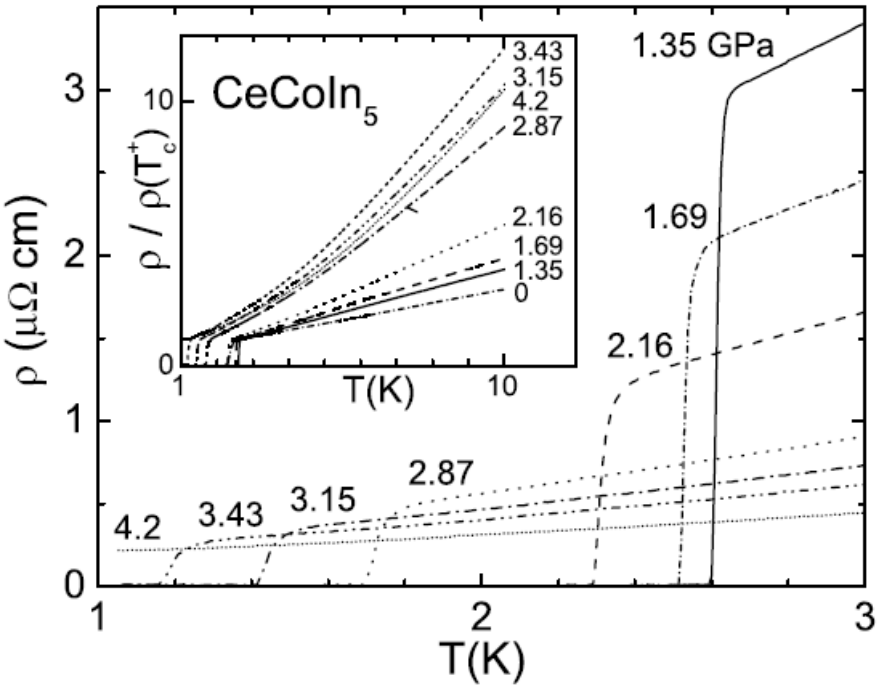

FIG. 1. Effect of pressure on the low-temperature resistivity and superconducting T_c of $CeCoIn_5$. The inset shows the resistivity ρ normalized by $\rho(T_c^+)$ up to 10 K.

Highest Tc
organic superconductors

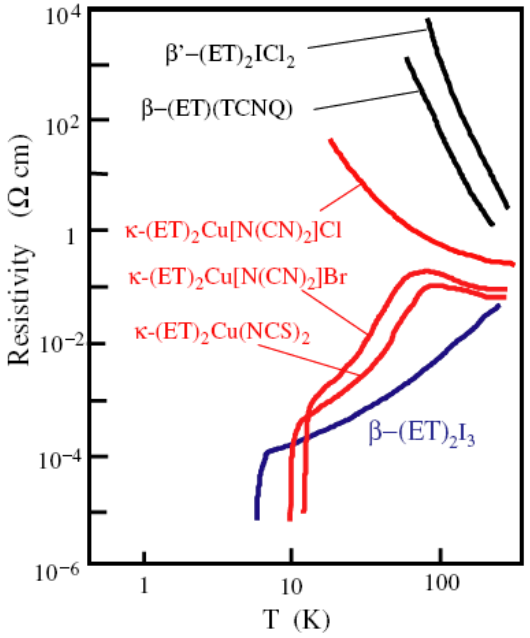

Fig. 2. (Color online) Resistivity behaviors of κ-$(ET)_2X$ and related dimeric compounds.